Frontiers in Bioscience Landmark

*Front. Biosci. (Landmark Ed)* **2026**; 31(8): 53657
https://doi.org/10.31083/FBL53657

*Original Research*

# Role of AMPK Signaling in the Neuroprotective Effects of Trehalose in Mice With a Pharmacological Model of Alzheimer's Disease

Alexander B. Pupyshev[1,*], Marina V. Ovsyukova[1], Anna A. Akopyan[1], Michael V. Tenditnik[1], Tatiana A. Korolenko[1], Nina I. Dubrovina[1], Maria A. Tikhonova[1]

[1]Laboratory of Experimental Neuroscience, Scientific Research Institute of Neurosciences and Medicine, 630117 Novosibirsk, Russia
*Correspondence: pupyshevab@neuronm.ru (Alexander B. Pupyshev)

Academic Editors: Antoni Camins and Hongquan Wang
Submitted: 7 May 2026 Revised: 3 July 2026 Accepted: 30 July 2026 Published: 21 August 2026

**Abstract**

**Background:** Trehalose (TRE) has demonstrated neuroprotective potential in models of Alzheimer's disease (AD)-like pathology and has been shown to activate AMP-activated protein kinase (AMPK) and induce autophagy in hepatocytes. The molecular mechanisms underlying the neuroprotective effects of TRE in the brain, including the involvement of AMPK signaling and autophagy, remain unclear. **Methods:** AD was modeled in C57BL/6 mice by intracerebroventricular administration of the amyloid-β (Aβ) fragment Aβ(25–35). The effects of TRE treatment (a 3% water solution in drinking water for 20 days) on AD-like pathology in the brain (frontal cortex, amygdala, and hippocampus) were assessed by immunohistochemical analysis, while cognitive function was evaluated using the passive avoidance test. AMPK activation was assessed by measuring AMPK (p-AMPK) levels in the brain and by evaluating the effects of its inhibitor dorsomorphin (DM; 10 mg/kg, i.p., 20 days, every other day for 20 days). **Results:** Aβ-treated mice exhibited markedly increased Aβ levels and neuroinflammatory responses in the brain, whereas levels of the autophagy marker LC3-II and p-AMPK were moderately reduced. TRE markedly reduced Aβ accumulation and neuroinflammation and restored cognitive performance to levels comparable to those of the Control group; it also increased LC3-II immunoreactivity and p-AMPK levels in the hippocampus and amygdala. DM did not abolish the neuroprotective effects of TRE but moderately inhibited AMPK in the hippocampus. **Conclusions:** Marked changes in brain Aβ levels and cognitive performance were not associated with either p-AMPK or autophagy marker levels, suggesting that additional mechanisms contribute to the neuroprotective effects of TRE in AD. Markers of autophagy initiation and AMPK activity responded similarly to AD modeling and TRE treatment and were positively correlated in the hippocampus, suggesting a role for AMPK in the regulation of TRE-induced hippocampal autophagy.

**Keywords:** Alzheimer's disease; mice; amyloid-β; brain; autophagy; trehalose; dorsomorphin; AMPK; LC3-II; passive avoidance test

## 1. Introduction

Neurodegeneration is closely associated with damage to cellular structures and the accumulation of aberrant proteins (α-synuclein, amyloid-β (Aβ), p-tau, etc.), which serve as markers of specific neurodegenerative diseases [1,2]. This accumulation is due to a weakening of the protein quality control system, including the ubiquitin-proteasome system and cytoprotective autophagy [3]. Alzheimer's disease (AD) is characterized by Aβ and p-tau accumulation and it is largely associated with decreased autophagy activity [4,5]. Accordingly, stimulation of autophagy produces a positive therapeutic effect on the course of experimental neurodegeneration, including AD models [6,7].

Autophagy is regulated by two pathways: mTOR-dependent and mTOR-independent [8,9]. In mice with a transgenic model of AD, both autophagy regulatory pathways appear to be impaired [10]. Moreover, activation of autophagy through both regulatory pathways has a positive effect on inhibiting neurodegeneration in both pharmacological and transgenic models of AD [8,11].

The weakening of mTOR-independent autophagy observed in AD-like pathology is largely associated with a decrease in the activity of the multimodal metabolic regulator AMP-activated protein kinase AMPK [12]. In transgenic mice of the 5xFAD (B6.Cg-Tg(APPSwFlLon,PSEN1M146LL286V)6799Vas/Mmjax) [13] and APP/PS1 (B6.Cg-Tg(APPswe,PSEN1dE9)85Dbo/Mmjax) [14] strains, the expression of p-AMPK in the brain was found to be significantly reduced, although this decrease is not always confirmed [15]. Normally, AMPK is activated in response to reduced energy supply, falling ATP levels. AMPK activation induces processes that restore energy supply, stimulate ATP production, suppress energy-consuming processes (including protein synthesis), reduce oxidative stress and neuroinflammation, induce autophagy, and generally inhibit neurodegeneration [16,17].

Disaccharide trehalose (TRE) was found to produce a stable neuroprotective effect on the one hand and to activate autophagy and AMPK on the other [11,18]. TRE's multimodal therapeutic activity includes: (1) chaperone-like properties for stabilizing protein folding, (2) activa-

**Copyright**: © 2026 The Author(s). Published by IMR Press.
This is an open access article under the CC BY 4.0 license.

**Publisher's Note**: IMR Press stays neutral with regard to jurisdictional claims in published maps and institutional affiliations.

tion of mTOR-independent autophagy, (3) stimulation of antioxidant cellular defense (including the Nrf2 factor), (4) inhibition of neuroinflammation. The therapeutic effect of TRE has been demonstrated in pharmacological and transgenic models of AD [11,19,20] and in aging mice [21]. Activation of autophagy, decreased levels of Aβ and p-tau, reduced neuroinflammation, attenuation of cognitive impairment, and inhibition of neuronal death have been observed.

The molecular target in the action of TRE on hepatocytes is the inhibition of the glucose transporter GLUT8, leading to energy deprivation and AMPK activation [22,23]. However, in the brain, the involvement of GLUT8 and AMPK in the induction of protective autophagy has not been convincingly confirmed [24]. Moreover, in the brain, the relationship between therapeutic activation of autophagy and AMPK activity is not always evident [17,18]. Typically, increased AMP/ADP levels in the brain activate ATP synthesis and suppress energy-consuming and anabolic processes [25].

However, AMPK activation may play a dual role depending on the disease stage: early activation of the kinase may inhibit neuroinflammation while chronic hyperactivation may exacerbate energy crisis and jeopardize neuronal viability [12,26]. A positive effect of autophagy and AMPK activation has been demonstrated in 5xFAD mice, a transgenic AD model, treated with crocetin [27], or in rats with middle cerebral artery occlusion treated with ezetimibe [28]. Furthermore, suppression of AMPK with the specific inhibitor dorsomorphin (DM) attenuated AMPK activation, reduced autophagy and the therapeutic effect [28]. AMPK is believed to mediate a link between energy metabolism disturbances and neuronal dysfunction and neurodegeneration, suggesting that energy deficits can lead to impairments in synaptic transmission and memory [29,30]. Thus, AMPK activation under these conditions may alleviate energy deficits and prevent the development of AD-like pathology. In other studies, such a connection is less clear. For example, TRE stimulated autophagy in the mouse brain but had no effect on p-AMPK expression, while exercise activated AMPK kinase but had no effect on autophagy [24]. A similar result was obtained in SH-SY5Y neuron-like cells *in vitro* [31]. It seems important to clarify the relation of the neuroprotective effect of TRE with the activation of AMPK and autophagy in brain neurons *in vivo*.

In this regard, we investigated the therapeutic effect of TRE on protection against AD-like pathology induced by intracerebroventricular (i.c.v.) administration of the amyloid fragment Aβ(25–35) in mice and its association with autophagy and p-AMPK levels in the mouse brain. The study aimed to reveal the involvement of AMPK activation and autophagy in the neuroprotective effects of TRE against AD-like pathology.

## 2. Methods

### *2.1 Animal Experiments*

Two-month-old male C57BL/6 mice (25–30 g) from the vivarium of the Scientific Research Institute of Neurosciences and Medicine (Novosibirsk, Russia) were used. The animals were maintained on a standard laboratory diet under standard conditions (light-dark cycle: 14 hours of light and 10 hours of darkness, temperature 20–22 °C, relative humidity 50–60%). Every effort was made to minimize the number of animals used and their suffering. All experimental procedures were carried out in accordance with international standards for the care and use of laboratory animals (NIH Guide, 2011). The study was approved by the Local Ethics Committee of the Scientific Research Institute of Neurosciences and Medicine (Protocol No. 1 dated January 19, 2023).

All animals were under veterinary control (including general external examination and body weight gain) during the experiment. The only criteria for exclusion were obvious health problems because of surgery or intermale fighting. All other clinically healthy male mice were included in the study. Criteria for inclusion: clinically healthy male mice of C57BL/6 strain, at an age of 2–2.5 m.o., and with body mass within 25–30 g. Each group was randomly formed (simple randomization by random number generator) into two cages of male C57BL/6 mice (N = 3–4 in each cage) obtained from the vivarium of the Scientific Research Institute of Neurosciences and Medicine (Novosibirsk, Russia). We did not mix mice from different cages because of high intermale aggression in C57BL/6 males. The initial N = 30. Five mice were excluded at an early period of the experiment (prior to behavioral testing) because of health problems (post-surgical complications; N = 2) or essential injury (because of high intermale aggression in C57BL/6 males; N = 3).

The animals were divided into four groups:

1. Control group: i.c.v. administration of vehicle (sterile water). Water intake ad libitum; intraperitoneal (i.p.) administration of DM vehicle (saline) every other day for 20 days (N = 6).

2. AD model (Aβ group): i.c.v. administration of Aβ(25–35). Water intake ad libitum; i.p. administration of saline every other day for 20 days (N = 7).

3. TRE treatment (Aβ+TRE group): i.c.v. administration of Aβ(25–35). Aβ-injected mice were given 3% TRE solution (as drinking) ad libitum for 20 days; i.p. administration of saline every other day for 20 days (N = 5).

4. AMPK inhibition (Aβ+TRE+DM group): i.c.v. administration of Aβ(25–35). Aβ-injected mice were treated with 3% TRE solution (as drinking) ad libitum for 20 days; i.p. injections of DM (10 mg/kg) every other day for 20 days. The rationale behind the DM dosage and treatment regimen adopted in the current study was based on previous reports [32] (N = 7).

The treatment with TRE and DM was started 2 days after the i.c.v. Aβ(25–35) administration. After the treatments, the animals were subjected to behavioral testing for 8 days, and then their brains were collected for immunohistochemical (IHC) analysis (see details below).

According to our previous results [33] and reports of other groups, N = 5–8 per group is enough to evaluate behavioral effects in the Open Field and Passive Avoidance tests (for the experimental design including 4 groups of comparison and a murine model of AD). N = 3–5 is enough to perform IHC analysis. We also checked the minimal number of animals per group using Power analysis and Interval estimation (STATISTICA 10.0 software (StatSoft, Tulsa, OK, USA)) using observed F from the previous studies, confidence level = 0.95, and power goal = 0.95.

Dr. Tenditnik, who was in charge of conducting the stereotaxic surgery and drug treatment, was aware of group allocation during the allocation, the conduct of the experiment, and biosampling. To minimise potential confounders, we mixed the order of cages during the behavioral testing and biosampling, i.e., we did not test 2 cages of a group successively but the 1st cages of each group, then the other 1st cages of each group.

The following reagents were used in the procedures: Amyloid Beta-Protein Fragment 25–35 (Aβ(25–35); Sigma-Aldrich, Darmstadt, Germany); D(+)-trehalose dihydrate (Tokyo Chemical Industry, Japan); Dorsomorphin (Compound C) (GLPBIO, China).

### *2.2 Pharmacological Model of AD*

A pharmacological model of AD induced by central injection of Aβ(25–35) was used. Aβ(25–35) preparation and the i.c.v. injections were performed according to previously published protocols [34]. The mice were anesthetized with the veterinary drug "Zoletil 100" (Virbac, France) in a dose of 40 mg/kg. A water solution of aggregated Aβ(25–35) oligomers or vehicle was injected bilaterally using a Hamilton syringe (25 µL, model 1702 RN SYR, needle size 22s ga, needle L 51 mm (2 inch)), a micropump, and Neurostar's Stereo Drive motorized stereotaxis system (Neurostar, Tübingen, Germany). The infusion rate was 1 µL/min; the needle was left at the injection site for an additional 5 min after the drug administration. A total of 10 µL (9.43 nmol) of the Aβ(25–35) solution or vehicle (sterile water) was administered bilaterally (by 5 µL into each lateral ventricle) to each mouse. The following coordinates from the mouse brain atlas were used [35]: AP = −0.46 mm; ML = ±0.9 mm; and DV = 2.5 mm from the bregma, midline, and skull surface, respectively.

### *2.3 Immunohistochemical (IHC) Analysis*

Mice were culled by $CO_2$ asphyxiation using a gradual fill method for pure (100%) $CO_2$ administration (a displacement rate from 30% to 70% of the chamber volume/min) according to the AVMA Guidelines for the Euthanasia of Animals (2020 edition). Then five randomly selected mice per group were transcardially perfused with phosphate-buffered saline (PBS), followed by 4% paraformaldehyde in PBS; then, their brains were rapidly removed and post-fixed in PBS containing 30% sucrose at 4 °C. After immersion in the embedding Tissue-Tek O.C.T. compound (Sakura Finetek, USA), the brains were frozen and stored at –70 °C until sectioning into 30-µm-thick slices on a cryostat, HistoSafe MicroCut – SADV (Citotest Scientific Co., Ltd., Nanjing, Jiangsu, China). Coronal slices along the frontal cortex [AP = 2.93 to 2.57 mm] or hippocampus [AP = −1.91 to −2.45 mm] of each mouse brain were prepared. Unstained brain sections were identified according to the mouse brain atlas [35]. The IHC analysis was performed according to a protocol described in detail previously [34]. We applied a rabbit polyclonal antibody (AF4650, Lot:56a9323, 1:100 dilution, Affinity Biosciences Ltd., China; https://www.affbiotech.com/) as a primary antibody to detect autophagosome marker LC3-II; a mouse monoclonal antibody (NBP2–13075, Lot: B-2, 1:1000 dilution, Novus Biologicals, Littleton, CO, USA) as a primary antibody to detect Aβ load; a rabbit polyclonal antibody (PAC288Mu01, 1:100 dilution, Cloude-Clone Corp., Wuhan, Hubei, China) as a primary antibody to detect IBA1; a rabbit polyclonal antibody against phospho-AMPK alpha (Thr172) (AF3423, Lot:49t6850, 1:200 dilution, Affinity Biosciences Ltd., China; https://www.affbiotech.com/) as a primary antibody to detect p-AMPK levels.

Fluorescently labeled Alexa Fluor 488 goat anti-rabbit IgG (ab150077, 1:600 dilution, Abcam, Cambridge, UK), and Alexa Fluor 568 goat anti-mouse IgG (ab175473, 1:400 dilution, Abcam, Cambridge, UK) antibodies served as the secondary antibodies. Finally, fluorescence images were captured with an Axioplan 2 (Carl Zeiss, Oberkochen, Germany) microscope and a confocal laser scanning microscope LSM 510 META (Carl Zeiss, Oberkochen, Germany) and then analyzed in Image Pro Plus Software 6.0 (Media Cybernetics, Rockville, MD, USA). Fluorescence intensity associated with the expression of specific proteins (Aβ or others) was measured as background-corrected integrated optical density (IOD) with subtraction of staining signals of the non-immunoreactive regions in the images converted to grayscale. For Aβ load, we also calculated the percentage of an area of interest occupied by Aβ aggregates. Fluorescence intensity of punctate LC3-II immunostaining was measured via subtraction of weak diffuse fluorescence of some areas (punctate staining vs. background staining of the nonpunctate regions) in the images converted to grayscale. The area of interest size was 18,208 $\mu m^2$ in the layer III of the frontal cortex, in the amygdala, or dentate gyrus of the hippocampus; 19,353 $\mu m^2$ in the CA1 area, or 26,100 $\mu m^2$ in the CA3 area of the hippocampus. The operator was blinded to the treatment assignment of images.

*2.4 Behavioral Testing*

Each mouse was handled for 5 min/day during two consecutive days before the behavioral testing. Prior to testing, a mouse was placed individually in a clean cage (25 cm × 40 cm × 20 cm) and transported to a dimly lit observation room (28 lux), with sound isolation reinforced by masking white noise of 70 dB. A test was started 10 min after establishing the habituation of a mouse to the testing conditions. The test equipment was cleaned with 20% ethanol and thoroughly dried before each test trial. As we performed objective observer-independent behavioral testing with automated systems (EthoVision XT 11.5 software, Noldus IT, Wageningen, The Netherlands) or Gemini Avoidance System (SanDiego Instruments, San Diego, CA, USA), blinding was not applicable.

2.4.1 The Open Field Test

This test was carried out to assess locomotor and exploratory activity and anxiety. The following parameters were measured: general locomotor activity by the total distance traveled (cm); anxiety by the time spent in the center of the arena; vertical locomotor activity and exploratory behavior by the number of rearing bouts. The test was performed in an open-top transparent Plexiglas installation with a square arena (40 × 40 × 37.5 cm) under bright illumination (1000 lux) from above. Mice were placed in the arena near the wall and their behavior was recorded for 10 min. Animal behavior was recorded using two digital video cameras PanasonicWV-CL930 (Panasonic System Networks Suzhou Co. Ltd., Suzhou, China) from the side and top. The video data were processed in the original EthoVision XT 11.5 software (Noldus IT, Wageningen, The Netherlands).

2.4.2 Passive Avoidance Test

Training on the passive avoidance reaction was performed by a standard single-session method in an experimental chamber with dark and light compartments and an automated Gemini Avoidance System apparatus (San Diego Instruments, CA, USA). Briefly, mice were habituated to the apparatus the day before passive avoidance acquisition. On the training day, mice were placed in the light compartment with the tail towards the open door. After transfer to the dark compartment, the door was closed and the mouse received a painful electric shock (0.5 mA, 2 s). After 30 s, the animal was transferred to the home cage. 24 h later, the mouse was again placed in the light compartment with the door opened for 300 s. The Gemini software Version 1.0.0 (SanDiego Instruments, San Diego, CA, USA) automatically recorded the latency to enter the dark compartment, and the data from the test served as a measure of acquisition of the conditioned passive avoidance response.

*2.5 Statistics*

The exact value of n in each experimental group was: Control (N = 6), Aβ (N = 7), Aβ+TRE (N = 5), Aβ+TRE+DM (N = 7) (for behavioral tests); Control (N = 3), Aβ (N = 3 for LC3, Aβ, and IBA1 assays; N = 4 for p-AMPK assay), Aβ+TRE (N = 3), Aβ+TRE+DM (N = 3) (for IHC analysis). STATISTICA 10.0 software (StatSoft, Tulsa, OK, USA) was used to perform all the statistical analyses. All the results are expressed as the mean ± SEM. The normality of the data distribution was determined by the Shapiro–Wilk W test; homogeneity of variance was checked using the Brown–Forsythe test. Statistical evaluation of data was performed: (1) by one-way analysis of variance (ANOVA) (results of IHC analysis) followed by Fisher's LSD post hoc test; (2) by repeated-measures ANOVA (results of the passive avoidance test; with the same group factor as for results of IHC analysis as between-subject variable and learning (training or test) as a repeated measure) followed by Fisher's LSD post hoc test; (3) by Kruskal–Wallis H test followed by multiple comparisons of mean ranks for all groups (results of the open field test). Correlation between LC3-II and p-AMPK expression was estimated using the $r$ Pearson correlation coefficient. Differences were considered significant at $p \leq 0.05$.

## 3. Results

*3.1 Effect of Trehalose and Dorsomorphin on Autophagic Activity in the Brain*

Autophagic activity was assessed using IHC analysis for the autophagy marker in the frontal cortex, amygdala, and hippocampus (Fig. 1). LC3-II is a marker of newly formed autophagosomes and hence its levels indicate the initial step of autophagy activation (autophagy initiation).

Significant differences between the groups were found in the hippocampal CA3 region [$F(3, 8) = 4.41$, $p < 0.05$], dentate gyrus (DG) [$F(3, 8) = 16.06$, $p < 0.001$], and amygdala [$F(3, 8) = 4.37$, $p < 0.05$].

LC3-II levels were reduced by approximately half in the Aβ group compared to the Control group in the hippocampal CA3 region, DG, and amygdala. TRE treatment totally restored LC3-II levels to values of the Control group; it caused approximately two–four-fold increase in the autophagy marker expression compared to the Aβ group in the CA3 region and DG of the hippocampus, and amygdala. DM significantly suppressed the autophagic marker compared to the Aβ+TRE group only in the DG ($p < 0.01$), although there was a tendency to decrease in the amygdala ($p = 0.15$) and CA3 area ($p = 0.2$). The results indicate that the DM inhibitory effect on autophagy associated with AMPK kinase inactivation was weak.

*3.2 Effect of Trehalose and Dorsomorphin on AMPK Activation*

In the study of AMPK activation, the levels of p-AMPK were assessed without reference to AMPK, since

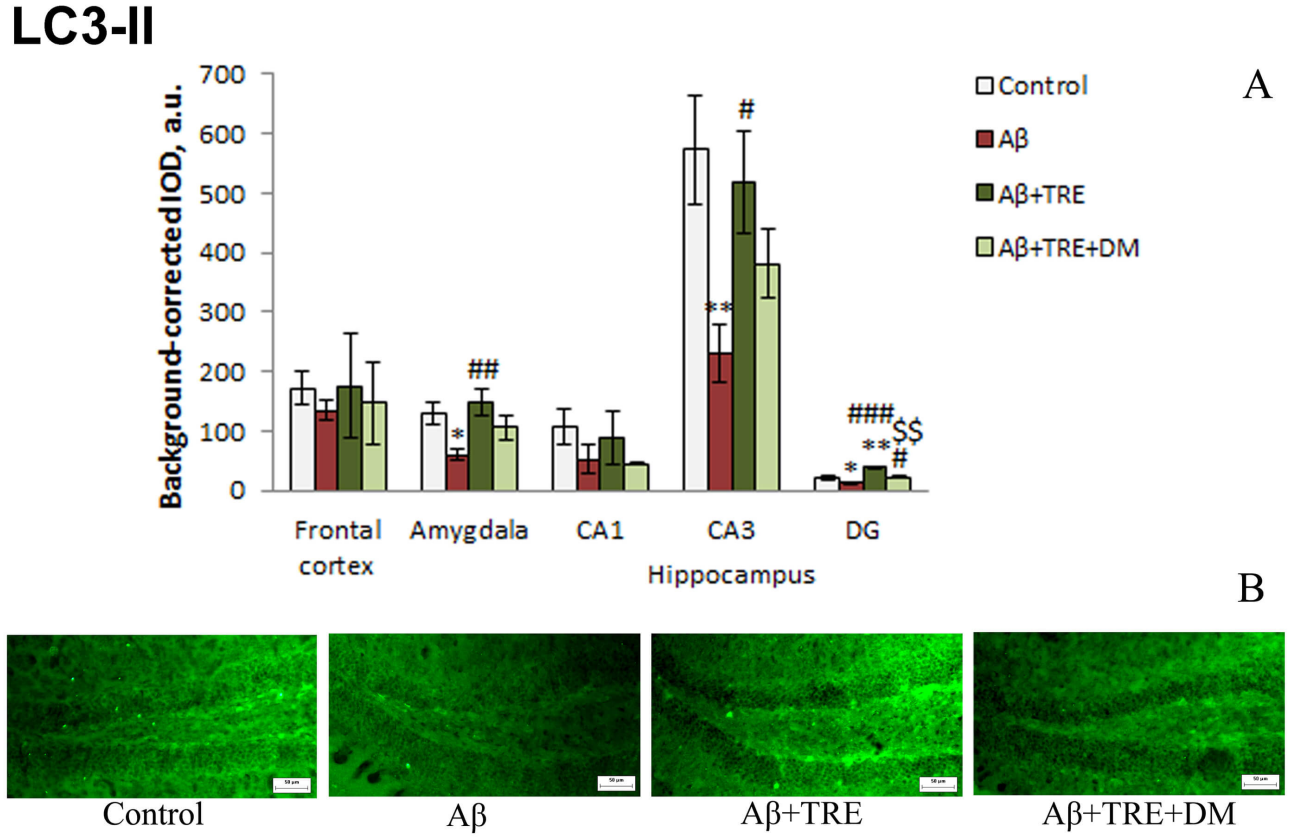


**Fig. 1. Effects of TRE (3% solution daily, 20 days) and DM (10 mg/kg, i.p., every other day, 20 days) on autophagy initiation in the brain in mice with Aβ-induced AD-like pathology**. To set up a pharmacological model of AD, mice were given bilateral i.c.v. injections of Aβ(25–35). The Control group received vehicle (sterile water) i.c.v. injections. The treatment with TRE and DM was started 2 days after the i.c.v. Aβ(25–35) administration. Abbreviations (hereinafter): CA1 – CA1 hippocampal area; CA3 – CA3 hippocampal area; DG – Dentate Gyrus. Groups (hereinafter): Control, i.c.v. vehicle administration; Aβ – AD model, i.c.v. administration of Aβ(25–35); Aβ+TRE – TRE treatment of mice with Aβ(25–35) administration; Aβ+TRE+DM – the combined treatment with TRE and DM of Aβ(25–35)-treated mice; a.u. – arbitrary units. (A) Quantitative results. The data are expressed as the mean ± SEM of the values obtained in an independent group of animals (n = 3 per group). Statistically significant differences: * $p < 0.05$, ** $p < 0.01$ vs. Control group; # $p < 0.05$, ## $p < 0.01$, ### $p < 0.001$ vs. Aβ group; $$ $p < 0.01$ vs. Aβ+TRE group. (B) LC3-II immunofluorescence in the DG of the hippocampus. Magnification: ×200, bar: 50 µm. TRE, trehalose; DM, dorsomorphin; DG, dentate gyrus.

the levels of total AMPK are usually stable [21]. Significant differences between the groups were found in the hippocampal CA3 region [$F(3, 9) = 4.24$, $p < 0.05$], DG [$F(3, 9) = 6.94$, $p < 0.05$], and amygdala [$F(3, 9) = 3.90$, $p < 0.05$] (Fig. 2). p-AMPK expression was generally reduced in the brain samples of the Aβ group compared to the Control group. TRE significantly enhanced p-AMPK expression in the brain. A substantial effect of TRE on p-AMPK expression was observed in the CA3 area ($p < 0.01$) and DG ($p < 0.01$) of the hippocampus and in the amygdala ($p < 0.05$) in comparison with the Aβ group.

In the hippocampal CA3 region, DG, and amygdala, TRE significantly restored p-AMPK expression up to Control group baseline levels, i.e., TRE treatment caused approximately a two-fold increase in p-AMPK levels compared to the Aβ group. This result could be considered as a significant effect of TRE on AMPK kinase activation. Moreover, co-administration of DM with TRE significantly inhibited the effect of TRE in the CA3 hippocampal area and DG (by approximately 40%). Notably, p-AMPK and LC3-II expression significantly correlated in the CA3 hippocampal area ($r = 0.619$, $p < 0.05$) and DG ($r = 0.664$, $p < 0.05$).

### *3.3 Expression of Amyloid-β in the Brain Upon the Treatment With Trehalose and Dorsomorphin*

To evaluate the impact of autophagy induction and AMPK activation in TRE neuroprotective effects, we measured the manifestation of AD-like deficits upon the treatment with TRE and DM. Aβ-accumulation was evaluated in the frontal cortex, amygdala, and hippocampus (Fig. 3). There were highly significant differences between the

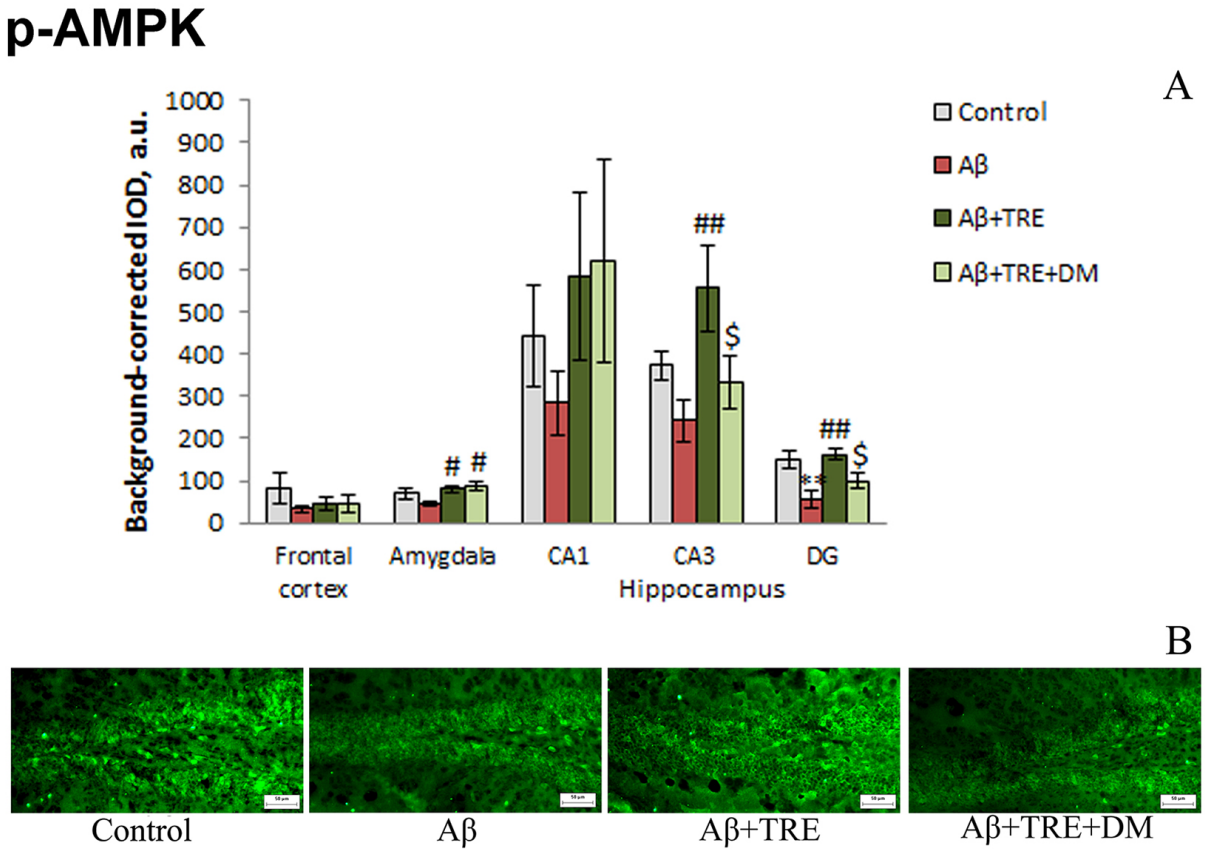


**Fig. 2. Effects of TRE (3% solution daily, 20 days) and DM (10 mg/kg, i.p., every other day, 20 days) on p-AMPK expression in the brain in mice with Aβ-induced AD-like pathology**. (A) Quantitative results. The data are expressed as the mean ± SEM of the values obtained in an independent group of animals (n = 3–4 per group). Statistically significant differences: ** $p < 0.01$ vs. Control group; # $p < 0.05$, ## $p < 0.01$ vs. Aβ group; $ $p < 0.05$ vs. Aβ+TRE group. (B) p-AMPK immunofluorescence in the DG of the hippocampus. Magnification: ×200, bar: 50 µm.

groups according to ANOVA both in the percentage of Aβ load area in the frontal cortex [$F(3, 8) = 272.41$, $p < 0.001$], CA1 hippocampal area [$F(3, 8) = 22.41$, $p < 0.001$], DG [$F(3, 8) = 31.03$, $p < 0.001$], and amygdala [$F(3, 8) = 112.71$, $p < 0.001$] and in Aβ IOD in the frontal cortex [$F(3, 8) = 20.77$, $p < 0.001$], CA1 hippocampal area [$F(3, 8) = 10.88$, $p < 0.01$], DG [$F(3, 8) = 8.61$, $p < 0.01$], and amygdala [$F(3, 8) = 21.54$, $p < 0.001$].

According to both indices (IOD and Aβ load area), Aβ levels were significantly higher in the Aβ group than in the Control group in the frontal cortex, CA1 area and DG of the hippocampus, and amygdala. Aβ load was significantly attenuated by TRE treatment in the frontal cortex, CA1 area and DG of the hippocampus, and amygdala. DM failed to reverse the positive effects of TRE in all the brain areas examined.

### *3.4 Effect of Trehalose and Dorsomorphin on Neuroinflammatory Response (Microglial Activation) Tested by IBA1 Expression*

Brain neuroinflammatory response was evaluated by microglial activation in the frontal cortex, hippocampus, and amygdala. The expression of the microglial marker IBA1 varied significantly between the groups in the frontal cortex [$F(3, 8) = 6.08$, $p < 0.05$], CA1 (SO) hippocampal area [$F(3, 8) = 11.41$, $p < 0.01$], DG [$F(3, 8) = 6.25$, $p < 0.05$], and amygdala [$F(3, 8) = 28.52$, $p < 0.001$] (Fig. 4). IBA1 levels were significantly augmented in Aβ group compared to the Control group in the frontal cortex, CA1 (SO) hippocampal area, DG, and amygdala, while TRE treatment significantly reduced the index down to levels in the Control group. DM failed to reverse the positive effects of TRE in all the brain areas examined.

### *3.5 Effect of Trehalose and Dorsomorphin on Behavioral Recovery*

#### 3.5.1 Passive Avoidance Test

The effects of TRE and DM on cognitive functions were studied using the passive avoidance test (associative learning and long-term fear memory). There were significant effects of the treatment factor [$F(3, 21) = 9.86$, $p < 0.001$], learning factor [repeated measures; $F(1, 21) = 104.27$, $p < 0.001$], and the interaction between these fac-

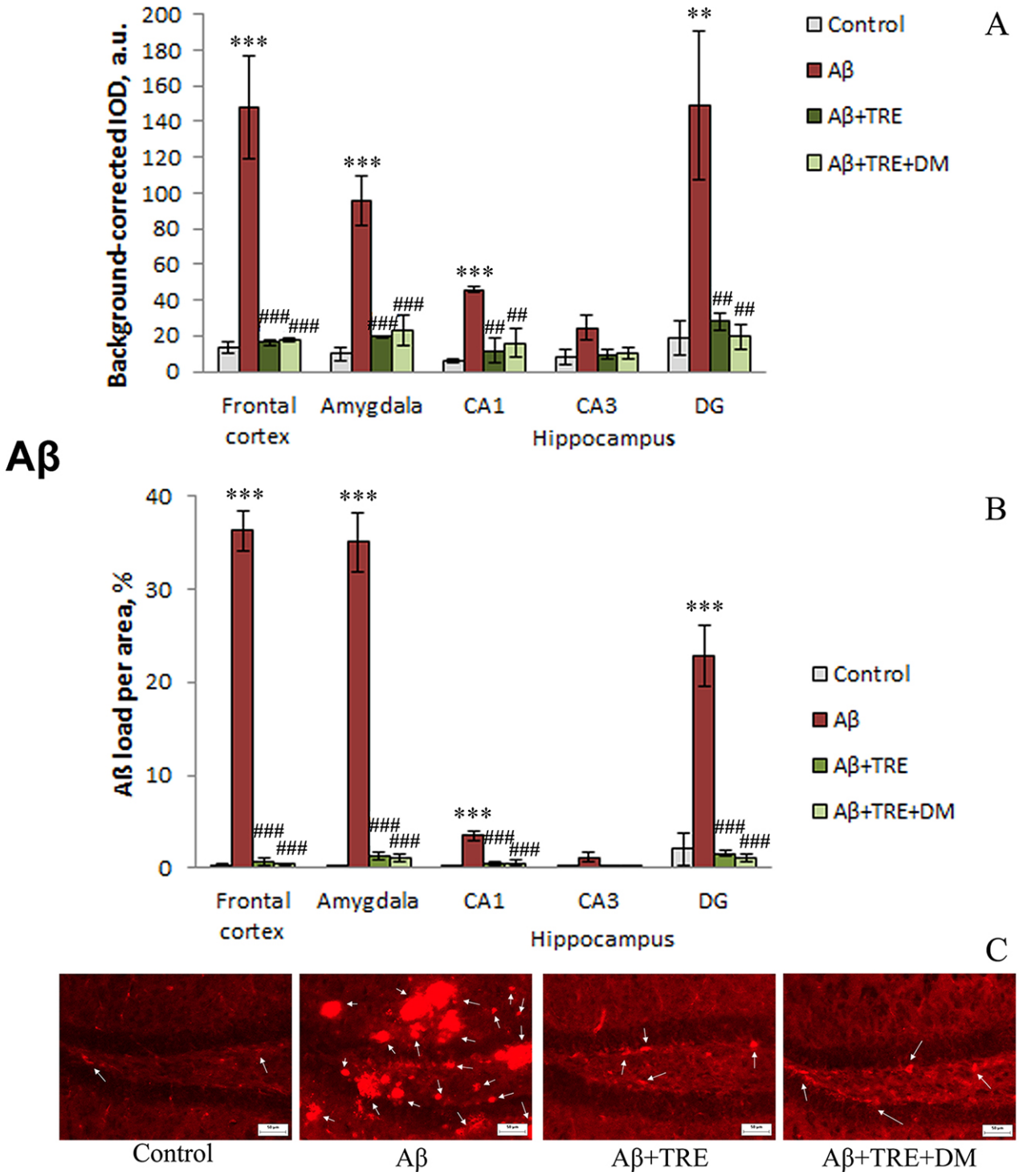


**Fig. 3. Effects of TRE (3% solution daily, 20 days) and DM (10 mg/kg, i.p., every other day, 20 days) on Aβ load in the brain in mice with Aβ-induced AD-like pathology**. (A) IOD (quantitative results). (B) Percentage of Aβ load per area (quantitative results). The data are expressed as the mean ± SEM of the values obtained in an independent group of animals (n = 3 per group). Statistically significant differences: ** $p < 0.01$, *** $p < 0.001$ vs. Control group; ## $p < 0.01$, ### $p < 0.001$ vs. Aβ group. (C) Aβ immunofluorescence in the DG of the hippocampus. Magnification: ×200, bar: 50 µm. White arrows indicate Aβ accumulation. In the Aβ group, large Aβ aggregates were revealed compared to weak intracellular signals in other groups. IOD, integrated optical density.

tors [$F(3, 21) = 8.12$, $p < 0.001$] on step-through latency in the passive avoidance test (Fig. 5). The latency of entering a dark compartment during training (prior to receiving an electric foot shock) did not differ significantly between the

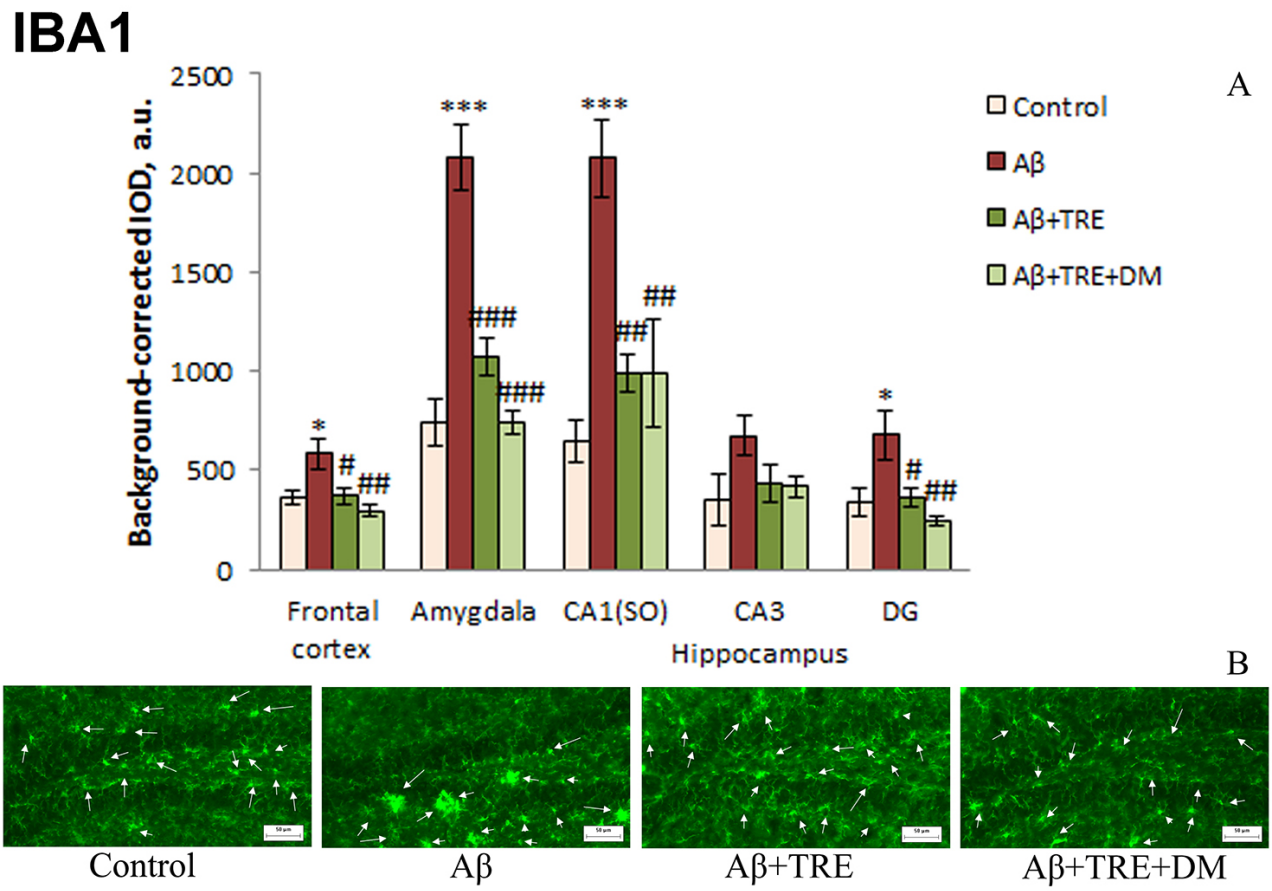


**Fig. 4. Effects of TRE (3% solution daily, 20 days) and DM (10 mg/kg, i.p., every other day, 20 days) on IBA1 expression in the brain in mice with Aβ-induced AD-like pathology**. (A) Quantitative results. The data are expressed as the mean ± SEM of the values obtained in an independent group of animals (n = 3 per group). Statistically significant differences: * $p < 0.05$, *** $p < 0.001$ vs. Control group; # $p < 0.05$, ## $p < 0.01$, ### $p < 0.001$ vs. Aβ group. Note: SO – stratum oriens, a layer where the basal dendrites of the neurons of the hippocampal CA1 area are located. (B) IBA1 immunofluorescence in the DG of the hippocampus. Magnification: ×200, bar: 50 μm. White arrows indicate microglial cells. In the Aβ group, activated microglia with a large soma and short branches were observed vs. microglia with a ramified morphology in other groups.

experimental groups. As evidence of learning on the test day, 24 h after receiving the foot shock, mice of the Control group demonstrated markedly longer step-through latency values than those on the training day ($p < 0.001$). In contrast, step-through latency on the test day was sharply lower in the Aβ-treated group than in the Control group ($p < 0.001$), thereby indicating memory impairment. TRE treatment produced a recovery of the learning and memory deficits, as evidenced by a significantly longer step-through latency on the test day compared to the Aβ-treated group ($p < 0.001$). DM did not block the restorative effect of TRE.

### 3.5.2 Open Field Test

The effects of TRE or TRE+DM co-administration were not associated with nonspecific effects on general locomotion or exploratory activity, since the open field test did not reveal significant differences between the groups in the distance traveled or the number of rearings (Table 1). The parameters of anxiety and emotionality also did not differ significantly between the groups.

Effect sizes and confidence intervals are listed in **Supplementary Table 1**. The descriptive statistics (mean ± SEM) for Figs. 1,2,3,4,5 are indicated in **Supplementary Table 2**.

## 4. Discussion

AD pathology is associated with progressive impairment of autophagy [4,5]. Importantly, autophagy is tightly related to the removal of aberrant Aβ and p-tau proteins [2,3]. Moreover, autophagy disturbances contribute in various ways to mitochondrial damage, energy deficiency, oxidative stress stimulation, neuroinflammation, regulatory imbalance, and other pathological processes [6,36]. Consequently, the activation of autophagy is recognized as a promising therapeutic approach in the treatment of experimental neurodegeneration [7,9]. As for the therapeutic ef-

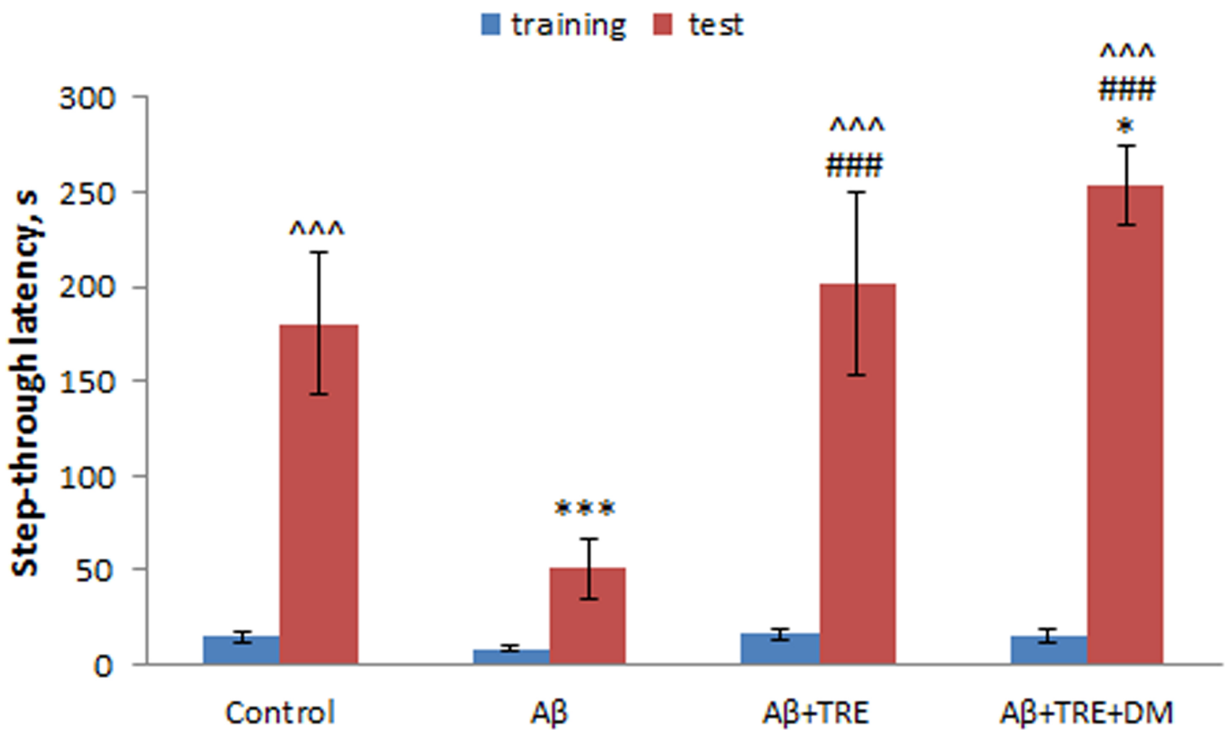


**Fig. 5. Effects of TRE (3% solution daily, 20 days) and DM (10 mg/kg, i.p., every other day, 20 days) on cognitive function (associative passive avoidance learning and fear memory) in mice with Aβ-induced AD-like pathology**. The data are expressed as the mean ± SEM of the values obtained in an independent group of animals (n = 5–7 per group). Statistically significant differences: ^^^ $p < 0.001$ vs. the values of the same group on training day; * $p < 0.05$, *** $p < 0.001$ vs. Control group; ### $p < 0.001$ vs. Aβ group.

**Table 1. Effects of TRE (3% solution daily, 20 days) and DM (10 mg/kg, i.p., every other day, 20 days) on behavior in the open field test in mice with Aβ-induced AD-like pathology**.

| Index | Group | | | | Kruskal-Wallis test |
|---|---|---|---|---|---|
| | Control | Aβ | Aβ+TRE | Aβ+TRE+DM | |
| Locomotor activity (distance traveled, cm) | 3563.4 ± 331.9 | 3383.5 ± 319.2 | 3727.5 ± 368 | 2568.7 ± 366 | H (3, N = 24) = 5.1; $p > 0.05$ |
| Exploratory activity (rearing, n) | 69 ± 13.9 | 65 ± 11.8 | 74 ± 13.3 | 43 ± 7.6 | H (3, N = 24) = 4.4; $p > 0.05$ |
| Anxiety (time in the center), s | 48.4 ± 9.9 | 54.4 ± 7.7 | 38.5 ± 4.1 | 48.3 ± 12.8 | H (3, N = 24) = 5.4; $p > 0.05$ |
| Emotionality (defecations, n) | 1 ± 0.4 | 2 ± 0.6 | 2 ± 1.5 | 1 ± 0.4 | H (3, N = 24) = 2.5; $p > 0.05$ |

Notes: The data are expressed as the mean ± SEM of the values obtained in an independent group of animals (n = 5–7 per group).

fect of TRE, the attention of researchers is mainly devoted to the mTOR-independent autophagy mechanism with the central link to AMP-activated protein kinase AMPK, which directly transmits a signal to the autophagy regulator ULK1.

In hepatocytes, AMPK is the main regulator of autophagy under the activation by TRE *in vitro* and *in vivo* [22,23,37], while autophagic activation by TRE via the GLUT8-AMPK-ULK1 pathway in neurons needs to be confirmed. At early stages of neuronal damage, AMPK stimulation produces a positive therapeutic effect on the restoration of hippocampal neurons and cognitive function. This effect is usually associated with the activation of neuroprotective autophagy [6,38,39]. Nevertheless, the involvement of AMPK in the therapeutic effect of TRE on neurodegeneration remains questionable.

Here, pharmacological modeling of AD resulted in a predominantly reduced autophagy in the brain, as evidenced by an approximately two-fold decrease in IHC levels of the LC3-II marker of the initial step of autophagy activation (autophagy initiation) in the amygdala, CA3 region, and DG of the hippocampus. This result is consistent with previous reports on decreased autophagy activity upon neurodegeneration [5]. In the present study, TRE treatment was accompanied by a significant increase in the autophagic marker and total restoration of its levels in the amygdala, CA3 region, and DG of the hippocampus. The observed recovery of the autophagy-related marker can be considered as a positive therapeutic effect. It should be noted that autophagy detection using the LC3-II marker is a combined indicator of both autophagy pathways, so it is not possible to distinguish the contribution of the mTOR-independent

pathway. The impact may be estimated only by AMPK activation, which is closely linked to the regulation of mTOR-independent autophagy [38].

AMPK activity in the brain was monitored using antibodies to the activated kinase p-AMPK without taking into account the baseline AMPK level, given that AMPK levels in the brain are typically stable and do not change significantly [21,40]. The AD modeling caused a general decrease in p-AMPK expression in the brain samples of the Aβ group compared to the Control group with a significant decrease in the DG. Overall, the decrease in p-AMPK expression in the brain of mice with AD-like pathology was less pronounced than the decrease in LC3-II levels, but the patterns of changes were similar. Moreover, both parameters responded positively and unidirectionally to TRE treatment. A significant, approximately two-fold increase in both parameters was observed in the amygdala, CA3 region, and DG of the hippocampus. Notably, p-AMPK and LC3-II expression significantly correlated in the CA3 hippocampal area and DG. Thus, TRE similarly regulated autophagy initiation and AMPK kinase activation, supporting the involvement of the GLUT8-AMPK-ULK1 pathway in autophagy induction in the brain by TRE treatment in mice with a pharmacological model of AD.

On the other hand, concerning the impact of autophagy initiation on the neuroprotective activity of TRE, it does not seem to be crucial. Indeed, TRE totally restored cognitive deficits (indices of associative learning and long-term fear memory) in Aβ-treated mice to levels of the Control group, which is consistent with our previous results on the effects of TRE on the recovery of cognitive function measured in the passive avoidance test in the models of AD and Parkinson's disease [41,42]. Amygdala, prefrontal cortex [43], and CA1 hippocampal area [44] are considered the main brain regions involved in learned fear. Aβ-induced cognitive impairment was associated with a pronounced accumulation of Aβ oligomers in the frontal cortex, amygdala, CA1 area and DG of the hippocampus in mice of the Aβ group. Moreover, a marked neuroinflammatory response (microglia hyperactivation), which is known to accompany Aβ load and aggravate Aβ oligomer-induced synaptic and neuronal deficits was also observed in the frontal cortex, amygdala, CA1 area and DG of the hippocampus in mice of the Aβ group. TRE treatment fully reversed these amyloid and neuroinflammatory alterations to the levels of the Control group, while moderate autophagy initiation under the TRE treatment was found only in the amygdala, CA3 area and DG of the hippocampus. Thus, the results do not provide evidence of a key role of TRE-induced autophagy induction in the anti-AD neuroprotective effects of TRE. Accordingly, it should be assumed that other cytoprotective mechanisms activated by TRE are also involved in the reduction of Aβ levels [11].

As we did not reveal a decisive contribution of autophagy initiation in the neuroprotective effects of TRE in the pharmacological Aβ-induced AD murine model, a significant impact of AMPK, a main regulator of mTOR-independent autophagy, on TRE therapeutic effects could not be expected. Indeed, the AMPK inhibitor DM had no effect on the indices of therapeutic anti-AD effect (Aβ load or cognitive recovery). On the other hand, AMPK inhibition confirmed the involvement of the AMPK-associated pathway in the autophagy induction by TRE treatment in the brain in mice with a pharmacological model of AD. DM suppressed autophagy initiation in the brain, although a significant decrease in LC3-II levels was revealed only in the DG. It should be noted that DM had no effect on the expression of p-AMPK in three brain regions (frontal cortex, amygdala, and CA1 hippocampal area), but it caused a significant reduction (by approximately 40%) in the CA3 region and the DG of the hippocampus. This result may reflect a limited attenuation of kinase activation by DM, which is likely to be insufficient for complete AMPK inhibition. Other studies have shown that i.p. administration of DM to mice also resulted in a slight inhibition of AMPK kinase in the brain (approximately 30%) [45], or a somewhat more pronounced effect [46]. It should also be noted that AMPK signaling is tightly involved in contextual fear memory formation [44]: a time-dependent decrease in AMPK activity was revealed after contextual fear conditioning in the CA1 but not CA3 area of the dorsal hippocampus. As all the mice in the present study underwent contextual fear conditioning in the passive avoidance test, oppositely directed effects of the behavioral testing procedure and experimental treatment might explain the absence of significant differences between the groups in p-AMPK levels in the CA1 hippocampal area. We may suggest that the regional differences observed in this study are related to differences in cell populations and neuron populations in particular and their sensitivity to TRE treatment due to alterations in the GLUT8–AMPK–ULK1 regulatory pathway signaling. Further research is needed to disclose these mechanisms.

## 5. Limitations

The limitations of the study include the limited evaluation of autophagy parameters, e.g., assays for autophagic flux were not applied. The autophagic marker LC3-II of newly formed autophagosomes applied here corresponds to the initial step of autophagy activation (autophagy initiation) and does not disclose further course of autophagy activation. Assay for AMPK activation was limited to measuring the p-AMPK levels and did not include evaluation of the levels of acetyl-CoA carboxylase-P, a substrate of activated AMPK, or other molecules of the GLUT8–AMPK–ULK1 regulatory signaling pathway. Differentiation of Aβ forms was not performed. Another limitation concerns sex-specific features and those related to familial forms of AD as these issues were beyond the scope of the study.

## 6. Conclusions

In sum, our results demonstrate a correlation between the activation of AMPK (by p-AMPK levels) and autophagy initiation (by LC3-II expression) in the hippocampus. TRE similarly regulated the autophagy induction and AMPK kinase activation, supporting the involvement of the GLUT8-AMPK-ULK1 pathway in autophagy induction by TRE treatment in the brain in mice with a pharmacological model of AD. A significant neuroprotective effect of TRE in eliminating Aβ accumulation and suppressing neuroinflammation in the frontal cortex, amygdala, and hippocampus as well as in restoring cognition was observed. At the same time, moderate TRE-induced autophagy and AMPK responses cannot fully explain the pronounced therapeutic effect of TRE solely through the activation of AMPK and/or autophagy initiation. Clearly, other mechanisms should be involved [11].

The AMPK inhibitor DM caused a significant reduction in p-AMPK levels (by approximately 40%) in the hippocampus (CA3 region and DG). Oppositely directed effects of the behavioral testing procedure (contextual fear conditioning) and experimental treatment on AMPK activity might explain the absence of significant differences between the groups in p-AMPK levels in the CA1 hippocampal area. DM suppressed autophagy initiation in the brain, although a significant decrease was revealed only in the DG. The results also support the involvement of the AMPK-associated pathway in autophagy induction by TRE treatment in the brain in mice with a pharmacological model of AD.

## Availability of Data and Materials

The datasets used and analyzed during the current study are available from the corresponding author on reasonable request.

## Author Contributions

ABP and MAT conceptualized and designed the research; MVT and NID performed the research; AAA performed an IHC analysis; MVO and TAK processed primary IHC data, analyzed the results, and designed figures; ABP, TAK, and MAT wrote and edited the manuscript; ABP and MAT - project administration and funding acquisition. All authors have read and agreed to the published version of the manuscript. All authors contributed to editorial changes in the manuscript. All authors have participated sufficiently in the work and agreed to be accountable for all aspects of the work.

## Ethics Approval and Consent to Participate

The study was approved by the Local Ethics Committee of the Scientific Research Institute of Neurosciences and Medicine (Protocol No. 1 dated January 19, 2023). All experimental procedures were carried out in accordance with international standards for the care and use of laboratory animals (NIH Guide, 2011). The study was carried out in accordance with the ARRIVE guidelines.


## Acknowledgment

We thank Konstantin S. Pavlov for technical support in behavioral testing and Eugenyi V. Nekhoroshev for experimental assistance.

## Funding

This study was supported by budget funding for fundamental scientific research of Ministry of Science and Higher Education of the Russian Federation for the Scientific Research Institute of Neurosciences and Medicine (theme no. 126020316369-9 (2026−2028)).


## Conflicts of Interest

The authors declare no conflicts of interest.

## Supplementary Material

Supplementary material associated with this article can be found, in the online version, at https://doi.org/10.31083/FBL53657.

## References


[1] Hansson O. Biomarkers for neurodegenerative diseases. Nature Medicine. 2021; 27: 954–963. https://doi.org/10.1038/s41591-021-01382-x

[2] Zhang H, Wei W, Zhao M, Ma L, Jiang X, Pei H, et al. Interaction between Aβ and Tau in the Pathogenesis of Alzheimer's Disease. International Journal of Biological Sciences. 2021; 17: 2181–2192. https://doi.org/10.7150/ijbs.57078

[3] Barmaki H, Nourazarian A, Khaki-Khatibi F. Proteostasis and neurodegeneration: a closer look at autophagy in Alzheimer's disease. Frontiers in Aging Neuroscience. 2023; 15: 1281338. https://doi.org/10.3389/fnagi.2023.1281338

[4] Uddin MS, Stachowiak A, Mamun AA, Tzvetkov NT, Takeda S, Atanasov AG, et al. Autophagy and Alzheimer's Disease: From Molecular Mechanisms to Therapeutic Implications. Frontiers in Aging Neuroscience. 2018; 10: 04. https://doi.org/10.3389/fnagi.2018.00004

[5] Li YY, Qin ZH, Sheng R. The Multiple Roles of Autophagy in Neural Function and Diseases. Neuroscience Bulletin. 2024; 40: 363–382. https://doi.org/10.1007/s12264-023-01120-y

[6] Zhao Y, Zhang Y, Zhang J, Zhang X, Yang G. Molecular Mechanism of Autophagy: Its Role in the Therapy of Alzheimer's Disease. Current Neuropharmacology. 2020; 18: 720–739. https://doi.org/10.2174/1570159X18666200114163636

[7] Zhang XW, Zhu XX, Tang DS, Lu JH. Targeting autophagy in Alzheimer's disease: Animal models and mechanisms. Zoological Research. 2023; 44: 1132–1145. https://doi.org/10.24272/j.issn.2095-8137.2023.294

[8] Sarkar S. Regulation of autophagy by mTOR-dependent and mTOR-independent pathways: autophagy dysfunction in neurodegenerative diseases and therapeutic application of autophagy enhancers. Biochemical Society Transactions. 2013; 41: 1103–1130. https://doi.org/10.1042/BST20130134

[9] Sose PM, Doshi GM, Kale PP. An Update on Autophagy as a Target in the Treatment of Alzheimer's Disease. Cur-

rent Drug Targets. 2023; 24: 547–567. https://doi.org/10.2174/1389450124666230417104325
[10] Park S, Park M, Lee HJ. Ginkgolide A enhances cognition and reduces amyloid-β by activating autophagy in the murine 5xFAD Alzheimer's disease model. Biomedicine & Pharmacotherapy = Biomedecine & Pharmacotherapie. 2025; 191: 118472. https://doi.org/10.1016/j.biopha.2025.118472
[11] Pupyshev AB, Klyushnik TP, Akopyan AA, Singh SK, Tikhonova MA. Disaccharide trehalose in experimental therapies for neurodegenerative disorders: Molecular targets and translational potential. Pharmacological Research. 2022; 183: 106373. https://doi.org/10.1016/j.phrs.2022.106373
[12] Yu L, Yang X, Lei HP, Hu YT, Wu LN, Zhou SY, et al. Multiple Mechanisms and Therapeutic Strategies for the Involvement of AMPK in the Development of Alzheimer's Disease. Molecular Neurobiology. 2025; 62: 15390–15409. https://doi.org/10.1007/s12035-025-05162-3
[13] Álvarez-Arellano L, Pedraza-Escalona M, Blanco-Ayala T, Camacho-Concha N, Cortés-Mendoza J, Pérez-Martínez L, et al. Autophagy impairment by caspase-1-dependent inflammation mediates memory loss in response to β-Amyloid peptide accumulation. Journal of Neuroscience Research. 2018; 96: 234–246. https://doi.org/10.1002/jnr.24130
[14] Wang X, Jia J. Magnolol improves Alzheimer's disease-like pathologies and cognitive decline by promoting autophagy through activation of the AMPK/mTOR/ULK1 pathway. Biomedicine & Pharmacotherapy = Biomedecine & Pharmacotherapie. 2023; 161: 114473. https://doi.org/10.1016/j.biopha.2023.114473
[15] Mary A, Barale S, Eysert F, Valverde A, Lacas-Gervais S, Bauer C, et al. Hampered AMPK-ULK1 cascade in Alzheimer's disease (AD) instigates mitochondria dysfunctions and AD-related alterations which are alleviated by metformin. Alzheimer's Research & Therapy. 2025; 17: 127. https://doi.org/10.1186/s13195-025-01772-0
[16] Yang L, Jiang Y, Shi L, Zhong D, Li Y, Li J, et al. AMPK: Potential Therapeutic Target for Alzheimer's Disease. Current Protein & Peptide Science. 2020; 21: 66–77. https://doi.org/10.2174/1389203720666190819142746
[17] Wang X, Zimmermann HR, Ma T. Therapeutic Potential of AMP-Activated Protein Kinase in Alzheimer's Disease. Journal of Alzheimer's Disease : JAD. 2019; 68: 33–38. https://doi.org/10.3233/JAD-181043
[18] Hosseinpour-Moghaddam K, Caraglia M, Sahebkar A. Autophagy induction by trehalose: Molecular mechanisms and therapeutic impacts. Journal of Cellular Physiology. 2018; 233: 6524–6543. https://doi.org/10.1002/jcp.26583
[19] Du J, Liang Y, Xu F, Sun B, Wang Z. Trehalose rescues Alzheimer's disease phenotypes in APP/PS1 transgenic mice. The Journal of Pharmacy and Pharmacology. 2013; 65: 1753–1756. https://doi.org/10.1111/jphp.12108
[20] Khalifeh M, Read MI, Barreto GE, Sahebkar A. Trehalose against Alzheimer's Disease: Insights into a Potential Therapy. BioEssays : News and Reviews in Molecular, Cellular and Developmental Biology. 2020; 42: e1900195. https://doi.org/10.1002/bies.201900195
[21] Pan S, Guo S, Dai J, Gu Y, Wang G, Wang Y, et al. Trehalose ameliorates autophagy dysregulation in aged cortex and acts as an exercise mimetic to delay brain aging in elderly mice. Food Science and Human Wellness. 2022; 11: 1036–1044. https://doi.org/10.1016/j.fshw.2022.03.028
[22] DeBosch BJ, Heitmeier MR, Mayer AL, Higgins CB, Crowley JR, Kraft TE, et al. Trehalose inhibits solute carrier 2A (SLC2A) proteins to induce autophagy and prevent hepatic steatosis. Science Signaling. 2016; 9: ra21. https://doi.org/10.1126/scisignal.aac5472
[23] Mayer AL, Higgins CB, Heitmeier MR, Kraft TE, Qian X, Crowley JR, et al. SLC2A8 (GLUT8) is a mammalian trehalose transporter required for trehalose-induced autophagy. Scientific Reports. 2016; 6: 38586. https://doi.org/10.1038/srep38586
[24] Narita H, Tanji K, Miki Y, Mori F, Wakabayashi K. Trehalose intake and exercise upregulate a glucose transporter, GLUT8, in the brain. Biochemical and Biophysical Research Communications. 2019; 514: 672–677. https://doi.org/10.1016/j.bbrc.2019.05.017
[25] Muraleedharan R, Dasgupta B. AMPK in the brain: its roles in glucose and neural metabolism. The FEBS Journal. 2022; 289: 2247–2262. https://doi.org/10.1111/febs.16151
[26] Shah SA, Amin FU, Khan M, Abid MN, Rehman SU, Kim TH, et al. Anthocyanins abrogate glutamate-induced AMPK activation, oxidative stress, neuroinflammation, and neurodegeneration in postnatal rat brain. Journal of Neuroinflammation. 2016; 13: 286. https://doi.org/10.1186/s12974-016-0752-y
[27] Wani A, Al Rihani SB, Sharma A, Weadick B, Govindarajan R, Khan SU, et al. Crocetin promotes clearance of amyloid-β by inducing autophagy via the STK11/LKB1-mediated AMPK pathway. Autophagy. 2021; 17: 3813–3832. https://doi.org/10.1080/15548627.2021.1872187
[28] Yu J, Wang WN, Matei N, Li X, Pang JW, Mo J, et al. Ezetimibe Attenuates Oxidative Stress and Neuroinflammation via the AMPK/Nrf2/TXNIP Pathway after MCAO in Rats. Oxidative Medicine and Cellular Longevity. 2020; 2020: 4717258. https://doi.org/10.1155/2020/4717258
[29] Peixoto CA, Oliveira WHD, Araújo SMDR, Nunes AKS. AMPK activation: Role in the signaling pathways of neuroinflammation and neurodegeneration. Experimental Neurology. 2017; 298: 31–41. https://doi.org/10.1016/j.expneurol.2017.08.013
[30] Liu YJ, Chern Y. AMPK-mediated regulation of neuronal metabolism and function in brain diseases. Journal of Neurogenetics. 2015; 29: 50–58. https://doi.org/10.3109/01677063.2015.1067203
[31] Benito-Cuesta I, Ordóñez-Gutiérrez L, Wandosell F. AMPK activation does not enhance autophagy in neurons in contrast to MTORC1 inhibition: different impact on β-amyloid clearance. Autophagy. 2021; 17: 656–671. https://doi.org/10.1080/15548627.2020.1728095
[32] Li F, Sun A, Cheng G, Liu D, Xiao J, Zhao Z, et al. Compound C Protects Against Cisplatin-Induced Nephrotoxicity Through Pleiotropic Effects. Frontiers in Physiology. 2020; 11: 614244. https://doi.org/10.3389/fphys.2020.614244
[33] Tikhonova MA, Amstislavskaya TG, Ho YJ, Akopyan AA, Tenditnik MV, Ovsyukova MV, et al. Neuroprotective Effects of Ceftriaxone Involve the Reduction of Aβ Burden and Neuroinflammatory Response in a Mouse Model of Alzheimer's Disease. Frontiers in Neuroscience. 2021; 15: 736786. https://doi.org/10.3389/fnins.2021.736786
[34] Belichenko VM, Bashirzade AA, Tenditnik MV, Dubrovina NI, Akopyan AA, Ovsyukova MV, et al. Comparative analysis of early neurodegeneration signs in a mouse model of Alzheimer's disease-like pathology induced by two types of the central (Intracerebroventricular vs. Intrahippocampal) administration of $A\beta_{25-35}$ oligomers. Behavioural Brain Research. 2023; 454: 114651. https://doi.org/10.1016/j.bbr.2023.114651
[35] Paxinos G, Franklin KBJ. Paxinos and Franklin's the Mouse Brain in Stereotaxic Coordinates. 4th edn. Elsevier/Academic Press: Amsterdam, Boston. 2013.
[36] Kuang H, Tan CY, Tian HZ, Liu LH, Yang MW, Hong FF, et al. Exploring the bi-directional relationship between autophagy and Alzheimer's disease. CNS Neuroscience & Therapeutics. 2020; 26: 155–166. https://doi.org/10.1111/cns.13216
[37] Pupyshev AB, Tikhonova MA. GLUT8- and AMPK-Dependent

Autophagy Signaling in the Mechanism of the Neuroprotective Action of Trehalose. Molekuliarnaia Biologiia. 2026; 60: 292–310. https://doi.org/10.7868/S3034555326020071

[38] Ge Y, Zhou M, Chen C, Wu X, Wang X. Role of AMPK mediated pathways in autophagy and aging. Biochimie. 2022; 195: 100–113. https://doi.org/10.1016/j.biochi.2021.11.008

[39] Nikbakhtzadeh M, Shaerzadeh F, Ashabi G. Highlighting the Protective or Degenerative Role of AMPK Activators in Dementia Experimental Models. CNS & Neurological Disorders Drug Targets. 2021; 20: 786–801. https://doi.org/10.2174/1871527320666210526160214

[40] He Z, Zhang H, Li X, Tu S, Wang Z, Han S, et al. The protective effects of Esculentoside A through AMPK in the triple transgenic mouse model of Alzheimer's disease. Phytomedicine : International Journal of Phytotherapy and Phytopharmacology. 2023; 109: 154555. https://doi.org/10.1016/j.phymed.2022.154555

[41] Pupyshev AB, Tikhonova MA, Akopyan AA, Tenditnik MV, Dubrovina NI, Korolenko TA. Therapeutic activation of autophagy by combined treatment with rapamycin and trehalose in a mouse MPTP-induced model of Parkinson's disease. Pharmacology, Biochemistry, and Behavior. 2019; 177: 1–11. https://doi.org/10.1016/j.pbb.2018.12.005

[42] Pupyshev AB, Belichenko VM, Tenditnik MV, Bashirzade AA, Dubrovina NI, Ovsyukova MV, et al. Combined induction of mTOR-dependent and mTOR-independent pathways of autophagy activation as an experimental therapy for Alzheimer's disease-like pathology in a mouse model. Pharmacology, Biochemistry, and Behavior. 2022; 217: 173406. https://doi.org/10.1016/j.pbb.2022.173406

[43] Silva F, Masella G, Madeira MF, Duarte CB, Santos M. TrkC Intracellular Signalling in the Brain Fear Network During the Formation of a Contextual Fear Memory. Molecular Neurobiology. 2023; 60: 3507–3521. https://doi.org/10.1007/s12035-023-03292-0

[44] Han Y, Luo Y, Sun J, Ding Z, Liu J, Yan W, et al. AMPK Signaling in the Dorsal Hippocampus Negatively Regulates Contextual Fear Memory Formation. Neuropsychopharmacology : Official Publication of the American College of Neuropsychopharmacology. 2016; 41: 1849–1864. https://doi.org/10.1038/npp.2015.355

[45] Zhang B, Zhang HX, Shi ST, Bai YL, Zhe X, Zhang SJ, et al. Interleukin-11 treatment protected against cerebral ischemia/reperfusion injury. Biomedicine & Pharmacotherapy = Biomedecine & Pharmacotherapie. 2019; 115: 108816. https://doi.org/10.1016/j.biopha.2019.108816

[46] Ammar RA, Mohamed AF, Kamal MM, Safar MM, Abdelkader NF. Neuroprotective effect of liraglutide in an experimental mouse model of multiple sclerosis: role of AMPK/SIRT1 signaling and NLRP3 inflammasome. Inflammopharmacology. 2022; 30: 919–934. https://doi.org/10.1007/s10787-022-00956-6